Quaternary Research 73 (2010) 304–312

Contents lists available at ScienceDirect

Quaternary Research

journal homepage: www.elsevier.com/locate/yqres

Climate change since 11.5 ka on the Diancang Massif on the southeastern margin of the Tibetan Plateau

Jiangqiang Yang [a,*], Wei Zhang [b], Zhijiu Cui [c], Chaolu Yi [a], Yixin Chen [c], Xiangke Xu [a]

[a] Key Laboratory of Tibetan Environment Changes and Land Surface Processes, Institute of Tibetan Plateau Research, CAS, Beijing 100085, China
[b] College of Urban and Environmental Sciences, Liaoning Normal University, Dianlian 116029, China
[c] College of Urban and Environmental Sciences, Peking University, Beijing 100871, China

ARTICLE INFO

Article history:
Received 25 August 2008
Available online 6 December 2009

Keywords:
Diancang Massif
Climate change
Indian Monsoon
Holocene

ABSTRACT

The Diancang Massif is located in a region linking the Tibetan and Yungui Plateaus. Climatically, it is in a transition belt between the south and middle subtropical zones, controlled by Indian monsoon and westerlies. Thus, this study provides more evidences on the evolution of Indian monsoon since the Holocene. We reconstruct the history of climate on the Diancang Massif since 11.5 ka, using integrated correlation of glacial activities, early human settlement sites, and climate proxies abstracted from variations in grain size, magnetic susceptibility, geochemical composition, and pollen in lacustrine sediments. Six climatic stages have been identified. Stage I, from 11.5 ka to 9.0 ka, is a relatively wet period, corresponding to the onset of the Holocene; from 9.5 ka to 6.0 ka, the climate is arid; a cold period follows from 6.0 ka to 5.3 ka, and this is succeeded by a temperate stage from 5.3 ka to 4.0 ka; from 4.0 ka to 0.73 ka the climate is again arid. Compared with other regions dominated by the Indian monsoon, there is a delay in response of the climate on the Diancang Massif to the onset of the Holocene.

Introduction

The Diancang Massif is located between the Tibetan Plateau and the Yungui Plateau, in a transition belt between the south and middle subtropical zones (Fig. 1). Along the southeast margin of the Plateau, the Massif is exposed to the northward intrusion of the Indian monsoon. In such a transitional belt both on terrains and on climate, the geological history of the Diancang Massif provides valuable information on local climate history and biological evolution. The study on the climate history of Diancang Massif will contribute on the understanding to the climate belts migration after the last glacial period, the correlation between the Tibetan Plateau and the Indian Ocean, as well as the evolution history, characteristics, impact on local environment and civilization of the Indian monsoon.

Research on glaciation of the Diancang Massif was initiated by Credner (1932), who suggested that a high stand of Lake Ximatan was a result of the last glacial period. About 60 yr later, Chen and Zhao, (1997) and Wan et al. (2005) surveyed the glacial landforms using aerial images and reported on them without field study. Still more recently, Yang et al. (2006, 2007) investigated these landforms and reconstructed the sequence of glacial advances since the last glacial period. In addition, a continuous climate record was constructed from lacustrine cores from Erhai Lake (Jiang et al., 1998; Zhou et al., 2003; Shen et al., 2005a, 2005b; Yang et al., 2005), a graben parallel to the east side of the Diancang Massif. Finally, the history of early settlements and cities on the eastern piedmont of the mountain were discussed by Zhang (1997).

Herein, we reconstruct the environmental changes since ~11.5 ka, the end of the last glacial period, based on glacio-lacustrine deposits, glacial stillstands, and archeological study of early settlement ruins.

Study area

The Diancang Massif (99°57′–100°12′ E, 25°36′–25°58′ N) is a ridge reaching over 4000 m above sea level (Fig. 1) with a length of 50 km and a width of 19 km. The city of Tali is located on the eastern piedmont of the mountain at an elevation of 1975 m. Tali receives 1040 mm of annual precipitation and enjoys a mean annual temperature of 15.0 °C. The climate of the Diancang Massif is characterized by an annual alternation of dry and wet seasons. The Indian Monsoon from the Bay of Bengal brings moisture from June to October and results in 850 mm precipitation each year; while during the rest of the year, the south branch of the westerlies, which shifts southward in the winter, brings dry air with an average precipitation of 190 mm.

The Diancang Massif lies within the subdomain of the *Pinus yunnanensis* and *Picea-Abies* forests of north Yunnan, which is part of the domain of semi-humid evergreen broad-leaved forest and *P. yunnanensis* forest of central and eastern Yunnan (Writing Group of Yunnan Vegetation, 1987). Four vegetation belts can be identified: an alpine belt (3800–4200 m *a.s.l.*), a sub-alpine belt (3400–3800 m

* Corresponding author.
E-mail address: jqyang@pku.org.cn (J. Yang).

0033-5894/$ – see front matter © 2009 University of Washington. Published by Elsevier Inc. All rights reserved.
doi:10.1016/j.yqres.2009.11.004

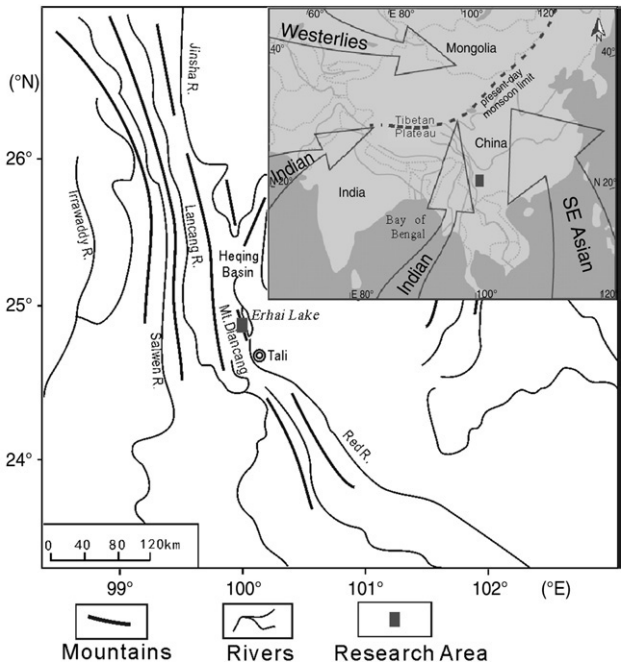

Figure 1. Location and climate system of the Diancang Massif. Atmospheric circulation is after Herzschuh (2006). The summer system is shown. At present, the westerlies shift southward in winter and are split by Tibetan Plateau. During the ice ages, the westerlies would have stayed south of the plateau throughout the year.

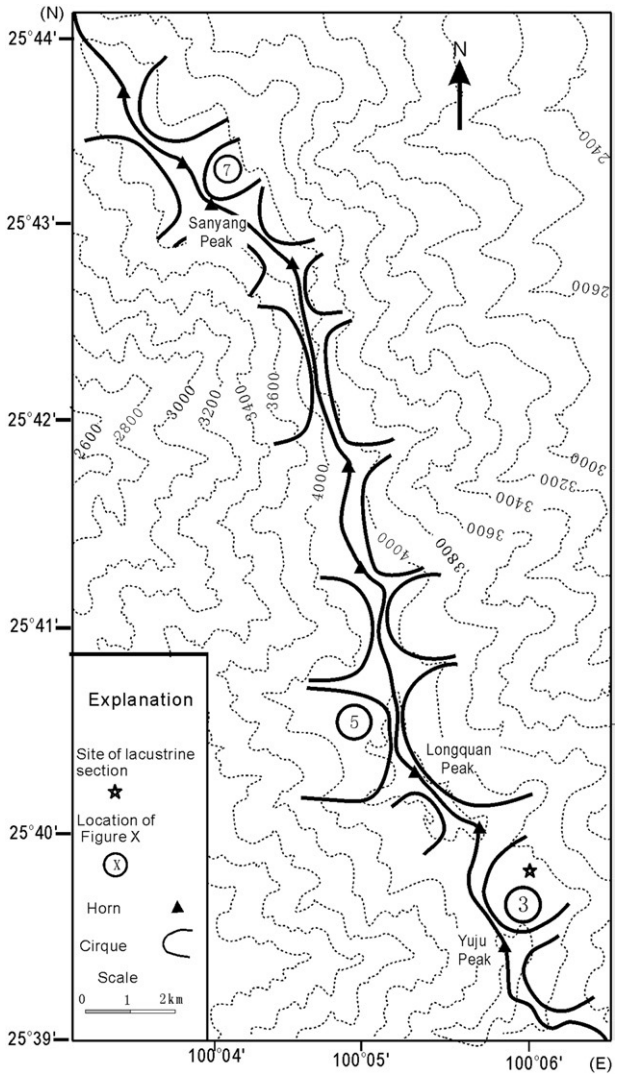

Figure 2. Cirques and study areas on the Diancang Massif.

a.s.l.), a middle-alpine belt (2600–3400 m *a.s.l.*) and a piedmont belt (2000–2600 m *a.s.l.*). The alpine belt is dominated by alpine cold meadows and coriaceous evergreen shrubs; the sub-alpine belt is composed of taiga such as *Abies* and *Picea*, alpine sclerophyll forest such as *Quercus* and coriaceous, and evergreen shrubs; the middle-alpine belt includes temperate mixed broadleaf-coniferous forest such as *Tsuga* and *Pinus*, temperate coniferous forest, shrubs and meadows; finally, the piedmont belt is dominated by heliophilic coniferous forest such as *Pinus* and *Ketteleria*, warm broadleaf forest of *Alnus nepalensis, Lithocarpus* and *Quercus*, and warm shrubs (Duan, 1995).

Study methods

The glacial landforms and deposits were investigated (Fig. 2) and relative ages were assigned in the field based on their positions, morphology, and state of preservation. Samples were collected and numerical ages of the glacial moraines were determined by TL, OSL and radiocarbon dating. The TL and OSL data is provided by the Institute of Geology, China Earthquake Administration and radiocarbon dating is provided by AMS Lab of Peking University (Yang et al., 2006).

Sampling

To obtain a continuous climate record, we exposed a 1.20-m lacustrine section in a desiccated glacial lake bed (100°05.99′ E, 25°06.08′ N) at an elevation of 3820 m *a.s.l.* (above sea level) on the north slope of Yuju Peak (Figs. 2 and 3). The 500 m^2 lake formed in a cirque dammed by an end moraine. Samples were collected at 25-mm intervals in aluminum boxes, and were analyzed for grain size, pollen spores, chemical components, and magnetic susceptibility. Four samples were taken for radiocarbon dating.

An ancient human settlement, Malong archeological site (100°09.76′ E, 25°39.65′ N), is located on an alluvial fan on the east slope of Malong Peak. Remains of two earthen walls are found at 2240 m and 2280 m *a.s.l.* These are considered to be defensive. Charcoal samples were collected from the bases of each wall for ^{14}C dating (Table 1).

In a maritime climate, glaciers can extend into forested areas. As a result, fine sediment with abundant datable organic material is transported from slopes and deposited in tills. We collected samples of the fine matrix of the tills for accelerator mass spectrometer (AMS) ^{14}C dating. To avoid contamination from roots of modern plants, all samples were collected at a depth of over 50 cm. Samples were sealed in plastic bags for later treatment.

Radiocarbon dating

The samples for radiocarbon dating were prepared by the Department of Archaeology at Peking University and were analyzed at the upgraded AMS facility of the University (PKUAMS) (Liu et al., 2000). Sample preparation followed the procedures described by Wu et al. (2000a and 2000b) and Yuan et al. (2000a and 2000b).

Analysis of lacustrine sediments

Low frequency magnetic susceptibility, χ_{lf}, was measured with a Bartington MS2 system. To identify the principal magnetic minerals in the lacustrine deposit, mineral compositions of two samples from the section and of one rock fragment from the catchment were analyzed by X-ray diffraction.

https://doi.org/10.1016/j.yqres.2009.11.004 Published online by Cambridge University Press

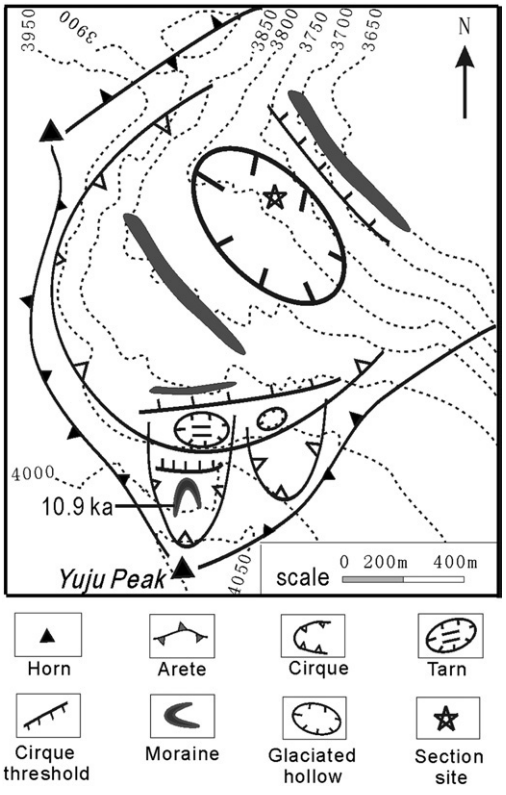

Figure 3. Glacial landforms and location of lacustrine section on the northern slope of Yuju Peak.

Pollen samples were prepared by standard methods using KOH, HF and acetolysis (Moore et al. 1999). The suspensions were sieved in an ultrasonic bath at 50 KHz on a 6 μm mesh, and stored in glycerine. *Lycopodium* spores were added as an exotic marker for calculation of pollen concentrations. A total of between 500 and 650 grains of pollen and spores were counted from each sample. Pollen and spore identification is based on Moore et al. (1991) and monographs (IBCAS, 1976; IBSCIB-CAS, 1982; Wang et al., 1995). The pollen diagram was expressed in concentration per gram.

Bulk samples of latchstring sediments were used for chemical analysis. Concentrations of SiO_2, MgO, K_2O, CaO, NaO, Fe_2O_3, Al_2O_3 and MnO were measured in a BAIRD ICP-2070 spectrometer. FeO was measured by titration with a $K_2Cr_2O_7$ solution. Grain sizes were determined using a Mastersizer 2000 laser particle size analyzer after organic matter and calcite were removed.

Results

Glacier advances after the last glacial period

Most of the glacial deposits and landforms are concentrated around peaks over 3500 m high (Fig. 2). Glacial landforms in three locations were investigated and dated.

Yuju peak

Four moraines are present on the northern slope of 4097-m Yuju Peak. The highest moraine, at 3960 m, is tongue-shaped and consists of 0.5–1.0 m boulders, with little soil and few plants. Till from the moraine was dated at 10.9 ka (Figs. 3 and 4) (Yang et al., 2006), so the moraine represents the glacial extent near the end of the last glacial period. (Unless otherwise stated, all ages are in calibrated years before present.) Lower moraines thus record the earlier glacial activities during the last glacial period.

Longquan peak

A series of glacial erosional and depositional landforms are preserved on the western slope of Longquan Peak (Figs. 5 and 6). The highest glacial landforms are a series of moraines, riegels and overdeepened basins above a small cirque threshold at 4010 m. An AMS radiocarbon date from a sample from the uppermost moraine, at 4041 m, was at 1490 cal yr BP. Two other samples were collected from moraines on the two riegels at elevations of 4021 m and 4012 m. Their ages were 3480 cal yr BP and 4410 cal yr BP respectively (Table 1). These ages imply that glacial advances or stillstands occurred in the middle Holocene and that ice then retreated gradually until 1490 cal yr BP, after which glaciers vanished completely.

On the northeast slope of Longquan Peak, there is a lake at 3950 m, dammed by a moraine. The altitude, orientation and scale suggest that the moraine originated from a hanging glacier. TL dating indicates a glacial advance or stillstand at 9.2 ka (Fig. 5) (Yang et al., 2006).

Sanyang peak

Sanyang Peak is 4019 m high, with four sets of glacier landforms preserved on its eastern slope (Figs. 7 and 8). The highest glacial relic is a small tongue-shaped moraine at 3985 m, which is dated at 1190 cal yr BP (Table 1). A 1500 m^2 ice-sculptured till-covered terrace lies below the moraine. AMS ^{14}C dating indicates the till was deposited at 5560 cal yr BP (Table 1).

Lithology and dating of the lacustrine deposits

The 1.2 m lacustrine section on Yuju Peak exposed six stages of differing lithology (Fig. 9). The base of the section, 1.00–1.20 m, consists of a layer of gray medium sand mingled with pebbles. This

Table 1
AMS radiocarbon dates from moraines, ancient settlement ruins, and the sediment from the glacio-lacustrine section on Yuju Peak.

Lab. code	Sample site (E, N)	Elevation (m)	Depth (cm)	Description	Measured (^{14}C yr BP)	Delta 13	Calibrated age	Average (cal yr BP)
BA02044	100°05.99′, 25°06.08′	3820	25	Organic silt in glacio-lacustrine section	810 ± 60	−23.78	1180 ~ 1270 AD	727
BA02047	100°05.99′, 25°06.08′	3820	47	Organic silt in glacio-lacustrine section	3,400 ± 80	−24.38	1900 ~ 1510 BC	3,650
BA02041	100°05.99′, 25°06.08′	3820	87	Organic silt in glacio-lacustrine section	7,270 ± 70	−25.00	6260 ~ 6000 BC	8,080
BA01035	100°05.99′, 25°06.08′	3820	112	Organic silt in glacio-lacustrine section	9,130 ± 110	−26.88	8640 ~ 8170 BC	10,350
BA022195	100°09.76′, 25°39.65′	2280	60	Charcoal in compacted earth of Malong settlement ruins, bottom of upper wall	2,890 ± 80	−24.15	1340 ~ 900 BC	3,070
BA022196	100°09.76′, 25°39.65′	2241	90	Charcoal in compacted earth of Malong settlement ruins, bottom of lower wall	3,440 ± 90	−24.58	1970 ~ 1520 BC	3,700
BA022208	100°05.69′, 25°40.10′	4041	50	Till in cirque on west slope of Longquan Peak	1,600 ± 110	−23.34	340 ~ 580 AD	1,490
BA022209	100°05.62′, 25°40.11′	4021	60	Till in cirque on west slope of Longquan Peak	3,240 ± 60	−24.66	1640 ~ 1410 BC	3,480
BA022210	100°05.56′, 25°40.11′,	4012	50	Till in cirque on west slope of Longquan Peak	3,960 ± 60	−24.41	2630 ~ 2284 BC	4,410
BA022204	100°04.28′, 25°43.40′	3985	50	Till in cirque on east slope of Sanyang Peak	1,310 ± 60	−23.90	640 ~ 880 AD	1,190
BA022205	100°04.31′, 25°43.40′	3941	50	Till in cirque on east slope of Sanyang Peak	4,830 ± 60	−24.71	3710 ~ 3500 BC	5,560

https://doi.org/10.1016/j.yqres.2009.11.004 Published online by Cambridge University Press

Figure 4. Glacial landforms on the northern slope of Yuju Peak (Photo: Jianqiang Yang).

underlies a gray silt layer, extending from 0.72 to 1.00 m. Gray medium and fine sand mingled with pebbles reappears from 0.62 to 0.72 m depth. A black, sticky bed of fine sand lies between 0.50 to 0.62 m. This is overlain by a gray medium and fine sand layer from 0.25 to 0.50 m. A layer of black soil, rich of organic matter, tops off the section. Table 1 provides both the measured radiocarbon dates and the calibrated ages that are used to establish the chronology of the section.

The particle size was determined by settling out of water and applying Stokes Law. Ages through the section were obtained by the interpolation between the two closest known time points, using the accumulation rate of the particles in 0.05–0.005 mm size range.

At the Malong archeological site, charcoal at the base of the lower wall was dated at 3700 cal yr BP, and that from the base of the upper wall was dated at 3050 cal yr BP (Table 1).

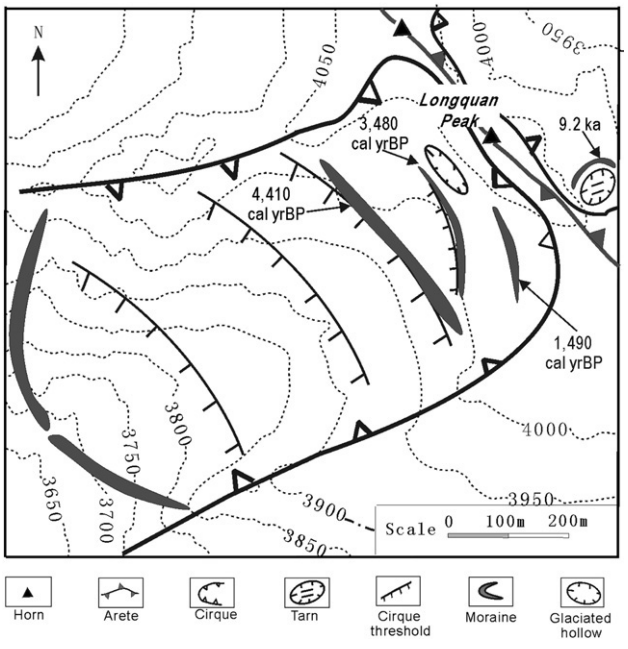

Figure 5. Glacial landforms and ages on the western and eastern slopes of Longquan Peak.

Laboratary analysis of lacustrine deposits

Interpretation of depositional proxies

Grain size. Based on the radiocarbon dating, lacustrine deposition in the lake below Yuju peak started at ~11.5 ka, which is close to the age of the highest moraine in the cirque, 10.9 ka. Therefore, it is reasonable that the glacier extended no further than the moraine at the beginning of lake sedimentation. The area of the lake catchment was 6000 m^2 and that of the glacier was 700 m^2. Thus, the ratio of the glacier area to the catchment area was always less than 1/9. This implies that the lake was supplied mostly by precipitation, not by glacier melt. Consequently, the grain size of the lacustrine deposits can be looked upon an indicator of precipitation in the catchment.

The relationship between grain size and precipitation varies with the time scale and local conditions (Chen et al., 2004). The lake is small and surrounded by steep moraines and rock cliffs, and the cold alpine climate restrains the development of dense vegetation. Thus, slope water from rain storms and melting of the snowpack plays an important role in sediment transportation. The particles in the catchment are easily transported during short periods of runoff and deposited after a short distance. In this situation, coarser deposits indicate more intense runoff and more humid conditions. Conversely, fine deposits imply less precipitation and a drier climate. Therefore the content of coarse sand is used as a proxy for precipitation.

Magnetic susceptibility. The difference between low- and high-frequency magnetic susceptibilities (χ_{lf} and χ_{hf}, respectively) is small, and both are positively correlated with the content of coarse sand and negatively correlated with the content of clay (Fig. 9). Thus, magnetic properties can be attributed to the coarse components. Mineralogical analysis shows a clear correlation between magnetic susceptibility and the content of Fe_2O_3 and FeO. Moreover, X-ray diffraction demonstrates that magnetite is the principal magnetic mineral in both the lacustrine deposits and the country rock. Hence, we conclude that magnetite is the main source of the magnetic signature of the lacustrine deposits. Magnetic susceptibility and the proportion of coarse sand are independent, and as both describe the input of mineral sediment, they both can be viewed as proxies of wetness in the catchment. We interpret the high values of χ and high concentrations of coarse sand as indicating a wet climate.

https://doi.org/10.1016/j.yqres.2009.11.004 Published online by Cambridge University Press

Figure 6. Glacial landforms on the western slope of Longquan Peak (Photo: Zhijiu Cui).

Geochemical components. In lakes, relatively high chemical deposition rates reflect active chemical weathering, while high physical deposition rates reflect low chemical and high physical weathering rates. The latter might be expected under cold, arid conditions. The ratio of the concentration of soluble elements to that of relatively insoluble ones, such as $SiO_2/(Al_2O_3+Fe_2O_3)$, and $(K_2O+CaO+Na_2O+MgO)/Al_2O_3$ are used as indices of the nature of the weathering. These will provide integrated records of temperature and humidity.

The concentrations of Fe and Mn in lacustrine deposits are controlled by the oxidation-reduction potential in the depositional environment. The binding ability of Mn to O_2 is much weaker than that of Fe to O_2, so Fe always deposits before Mn as climate becomes drier and the lake surface falls. Therefore, high Fe/Mn ratio indicates an arid climate (Luo and Chen, 1998; Tan and Yu, 1999).

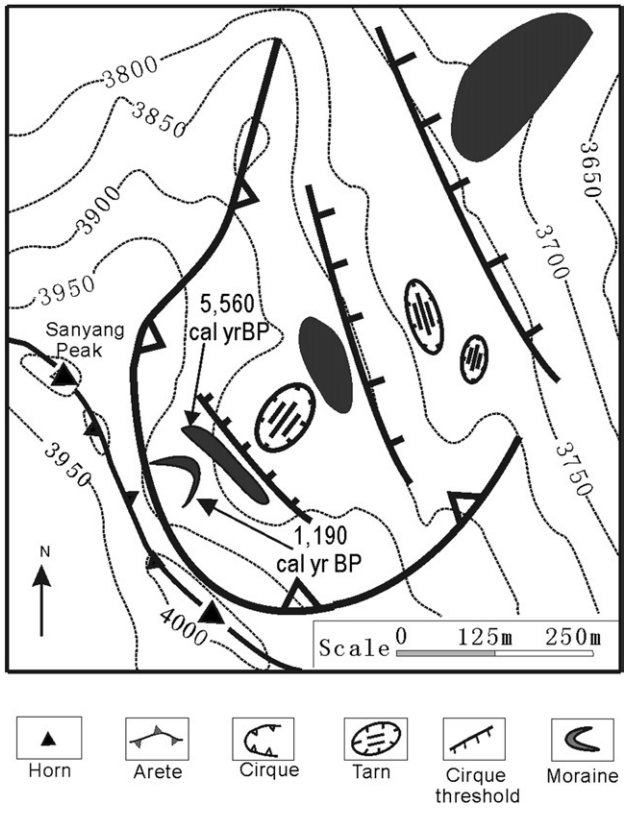

Figure 7. Glacial landforms and ages on the eastern slope of Sanyang Peak.

Variations of environmental proxies in the sedimentary profile

Figure 9 shows the changes in lithology grain size, low frequency magnetic susceptibility (χ_{lf}), geochemical ratios, and pollen species with depth in the excavated lacustrine section.

Stage I, from 1.20 to 1.00 m, is believed to have been deposited between 11.5 and 9.5 ka. As the clay content (hereafter referred to as CC) decreases from 1.3% to 0.7%, the content of coarse sands (CCS) increases from 2.1% to 9%. χ_{lf} shows a trend from 127 to 716, rising in conjunction with the increase of grain size and quickly reaching a persistent high. The ratio of K + Na + Ca + Mg to Al (KNaCaMg/Al) fluctuates from 1.0 to 1.1, and the ratio of Si to Al + Fe (Si/AlFe) fluctuates between 3.2 and 2.8. The Fe/Mn ratio remains low, between 35 and 43. Pollen analysis suggests an abundance of broad-leaved vegetation, such as *Betula*, *Alnus*, *Carpinus* and *Juglans*. The concentration of conifers remains relatively low. However, the conifers clearly increase at the expense of broad-leaved trees in the late part of stage I.

From 1.00 to 0.72 m depth (~9.5–6.0 ka), Stage II, CCS declines to 4.5% and the CC increases to 0.8%, consistent with the decline of χ_{lf} from 720 to 411. Si/AlFe shows a tiny decrease from 2.8 to 2.6 at 8.1 ka, followed by a gradual increase to 3.3, as the ratio KNaCaMg/Al declines to ~1.0, then grows to nearly 1.2. After remaining consistently low from ~9.5 to ~7.8 ka, Fe/Mn increases abruptly to its highest value, 143, at 7.5 ka. The pollen content changes at 8.1 ka: before this time, all species, including trees and herbs, decrease markedly. After 8.1 ka, herbs, broad-leaved trees and conifers such as *Tsuga*, *Ketelleria* and *Pinus* increase to their maximum Holocene values, while *Abies* and *Picea* continue falling and vanish at 7.0 ka.

From 0.72 to 0.62 m depth (~6.0–5.3 ka), Stage III, broad-leaved trees and the conifers *Tsuga*, *Ketelleria* and *Pinus* decline, while *Abies* and *Picea* come back. During this period, CCS is low with a minimum value of 3.4%, and CC displays a peak value of 1.2%. Meanwhile, χ_{lf} remains low with an average value of ~200. Si/AlFe reaches a minimum value of 2.3 and Fe/Mn returns to low values, averaging ~40.

From 0.62 to 0.50 m depth (~5.3–4.0 ka), Stage IV, χ_{lf} reaches its highest value of 801 and CCS increases to another high of 6.8%, while CC begins to decrease. Both Si/AlFe and KNaCaMg/Al increase notably. Herbs and tree pollen, especially that of broad-leaved trees, show revivals. *Keterleria* begins to appear for the first time.

From 0.50 to 0.25 m depth (~4.0–0.73 ka), Stage V, CCS displays a pair of troughs and CC continues a gradual rise, along with a distinct drop in the χ_{lf} values. The ratios of Si/AlFe and Ca/MgAl remain consistently high, with averages of 3.2 and 1.2, respectively. Fe/Mn increases dramatically and remains distinctively high. Herb pollen becomes relatively low. Almost all the tree species decrease gradually and finish low contents. *Abies*, *Picea*, *Bettula*, *Alnus*, *Carpinus* almost disappear.

https://doi.org/10.1016/j.yqres.2009.11.004 Published online by Cambridge University Press

Figure 8. Glacial landforms on the eastern slope of Sanyang Peak (Photo: Jianqiang Yang).

In the top 0.25 m (~0.73 ka to the present), Stage VI, Fe/Mn drops to a minimum of 21. Both CCS and χ_{lf} increase irregularly, with averages of 6.8% and 400%, respectively. CC varies with an average of 1.2. Except for small quantities of *Abies, Pinus* and *Ketelleria,* all trees and herbs are extremely low.

Discussion

Climate change on the Diancang Massif since the Holocene

Based on the correlation of glacial lacustrine deposits, glacial history, and evidence of human activities, we can reconstruct changes in climate of the Diancang Massif during the Holocene.

During Stage I (11.5 to 9.5 ka), the increases in both CCS and magnetic susceptibility suggest strengthened precipitation. The lake started form, largely supplied by the increasing rainfall. The noteworthy expansion of broad-leaved forests indicates a warm period. In Erhai Lake, an abundance of *Betula* and an increase in *Tsuga* also suggest similar conditions (Shen et al., 2005a). The dominance of broad-leaved trees reveals that the lake site is relatively close to the sub-alpine forest vegetation zone. In view of this apparent relative warmth, the pause in glacier retreat long enough to build the 10.9 ka moraine on the north flank of Yuju Peak must be attributed to intensified precipitation. This is consistent with Thompson et al.'s (2006) conclusion that the mass balance of glaciers in the southern and central mountains of the Tibetan Plateau is controlled primarily by moisture availability rather than by temperature. In summary, warm weather and relatively high precipitation are the climatic characteristics of this stage.

Stage II (9.5 to 6.0 ka) is characterized by relative dryness. Two substages can be identified: Substage IIa (9.5 to 8.5 ka) starts with cool conditions and gradually becomes arid; this is indicated by the decline in the pollen of all the woody plants. The decrease in tree species, especially broad-leaved species, implies a decrease in elevation of the treeline. The decrease in temperature could also have resulted in the ~9.2 ka moraine on the east slope of Longquan Peak. In Substage IIb (8.5 to 6.0 ka), the increase in both tree and herb pollen suggests that the climate became progressively warmer. The period from 8.5 ka to 6.8 ka appears to be the optimum during the Holocene. The decrease in *Abies* and *Picea* and the increase in broad-leaved forests suggest

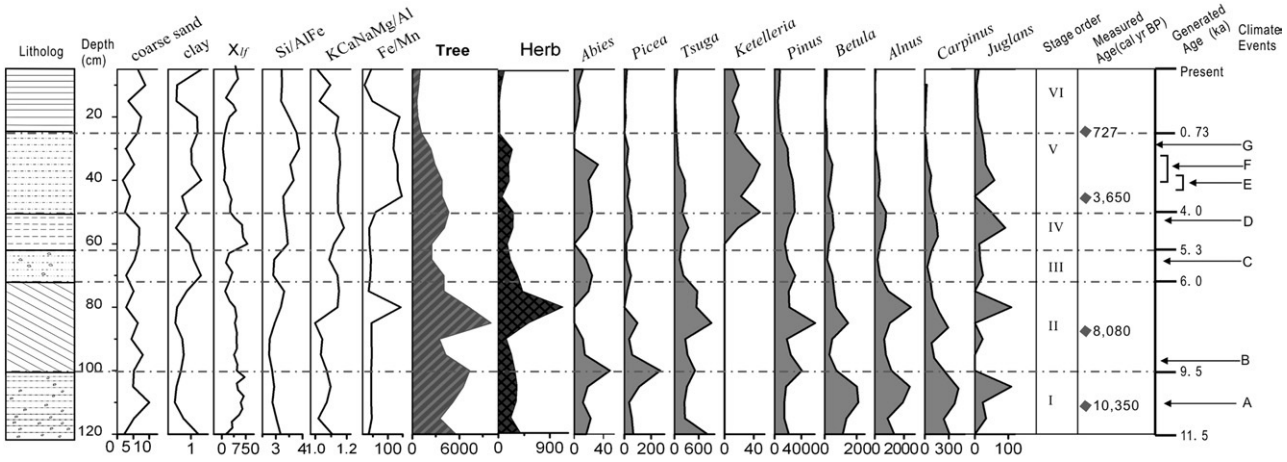

Figure 9. Holocene climate history record from lacustrine section on Yuju Peak, based on sedimentary log, grain size, magnetic susceptibility, geochemical components, pollen, and climate events. The Climate events are: (A) Glacial advance at 10,900 ± 800 yr BP on the north floor of Yuju Peak; (B) Glacial advance at 9200 ± 730 yr BP on the east floor of Longquan Peak; (C) Glacial advance at 5560 cal yr BP on the east floor of Sanyang Peak; (D) Glacial advance at 4410 cal yr BP on the west flank of Longquan Peak; (E) Human activities between 3700 and 3070 cal yr BP; (F) Glacial recession at 3480 cal yr BP and disappearance after 1490 cal yr BP on the west flank of Longquan Peak; (G) Glacial disappearance after 1190 cal yr BP on the east flank of Sanyang Peak.

https://doi.org/10.1016/j.yqres.2009.11.004 Published online by Cambridge University Press

that, in response to the favorable environment, the treeline rose again. On the other hand, the increases in Si/AlFe and KCaNaMg/Al as well as the peak in Fe/Mn imply that it is still dry.

During stage III (6.0 to 5.3 ka) the relative increase in coniferous forests and decline in broadleaf forests suggests that the climate turned colder. Under such hard conditions, the accumulation of both woody and herbaceous plants in the sediments deposited in Erhai Lake fell dramatically (Zhou et al., 2003). The low temperature led to the decline in vegetation and the glacier advance on the eastern slope of Sanyang Peak at about 5560 cal yr BP. The low values of CCS and magnetic susceptibility imply dry conditions.

Stage IV (5.3 to 4.0 ka) appears to have been a period of moderate climate in the Diancang Massif. High CCS values and low Ca/MgAl ratios indicate a wet climate and deep water in the lake on Yuju Peak. The recovery of broad-leaved forests, especially the presence of *Ketelleria*, indicates warm conditions and a possible increase in elevation of the treeline. The glacier advance at about 4.4 ka on the western slope of Longquan Peak may have resulted from a combination of high precipitation and moderate temperatures.

During Stage V (4.0 to 0.73 ka), all the proxies suggest an arid environment that culminated at 1.2 ka. The glacial retreat from 3480 to 1490 cal yr BP is recorded by the two uppermost moraines on the western slope of Longquan Peak. The youngest moraine on the eastern slope of Sanyang Peak is dated at 1190 cal yr BP, which suggests that a glacier persisted here during much of this arid period, but vanished near the end of it. Pollen evidence indicates that woody plants, including almost all the coniferous and broad-leafed forest species, decreased gradually. This implies that the treeline migrated downward. No *Picea* or *Abies* is found in the lacustrine sediments from Erhai Lake as lake levels declined (Zhou et al., 2003).

The earliest records of human activity in the research area were found during Stage V. Radiocarbon ages of the charcoal at the bases of the defensive walls of the Malong relic site indicate that the walls were built between 3070 and 3697 cal yr BP (Table 1). At that time, lacustrine sediments exposed on the piedmont indicate that the level of Erhai Lake was 2200 m *a.s.l* (Zhang, 1997). As the climate became drier, the level of Erhai Lake declined and humans gradually migrated from the piedmont to the basin. Archaeological research shows that during the Han and Jin Dynasties (2.1 to 1.7 ka) settlements were located at 2200–2000 m, and during the Tang and Song Dynasties (1.3 to 0.8 ka) cities were built at 2000–2100 m. People began to settle below 1975 m only after the Yuan dynasty (0.73 ka) (Zhang, 1997). Therefore, the falling lake surface and the resulting human migration, corresponding in time to the glacial retreat, are the result of, and evidence for an arid climate.

High values of CCS and magnetic susceptibility, low values of Si/FeAl and KCaNaMg/Al, and relatively high percentages of coniferous trees suggest that the climate became wet again after 0.73 ka (Stage VI). However, the overall concentration of vegetation is low, which may be attributable to increasingly destructive human activities (Shen et al., 2005a).

Local climate change and the evolution of the Indian monsoon

The onset of the Holocene

The glacial lake on Yuju Peak originated at 11.5 ka. This marks the end of the Younger Dryas and beginning of the Holocene. This climate change coincides with similar climate events in neighboring regions, such as the dramatic decrease in $\delta^{18}O$ at ~11.5 ka in stalagmite calcite in southwest China (Dykoski et al., 2005), and the transition to deposition of red sediment at 12 ka in Qinghai Lake (Ji et al., 2005). Morrill et al. (2003) identified some broad-scale and abrupt changes in summer monsoon intensities at ~11.5 ka, which are recorded across both the southwest and southeast Asian monsoon zones.

In fact, the local responses to the intensification of Indian monsoon are not exactly synchronous; the change appears to have been a little earlier in western regions, closer to the source of the monsoon moisture. Sediments in the Arabian Sea show that a strong and persistent Asian Heat Low developed during the boreal summer (Sirocko et al, 1993) and the Indian Monsoon intensified around 13.0–12.0 ka (Leuschner and Sirocko, 2003). Reduced percentages of eolian terrigenous sediment in a core from Hole 658C, West Africa, suggest that a humid period started at 14.8 ka (DeMenocal et al., 2000a).

In contrast, climate events indicating the start of the Holocene on Tibetan plateau occurred later. In Cuoe Lake in the central Tibetan plateau, TOC and Sr concentrations did not increase until 10.1 ka (Wu et al., 2006), and basal ages of the Puruogangri and Dasuopu ice caps suggest that the intensified Asian monsoon circulation brought more precipitation to the plateau around 9 ka (Thompson et al., 2006). In Sumxi Co on the western plateau, high lake levels and the expansion of *Artemisia* steppe occurred at ~10 ka (Gasse et al., 1991); this is inferred to be the onset of the Holocene there. Similarly, the incision of Sutlej River in the northwest Himalaya began at ~10 ka (Bookhagen et al., 2006).

The asynchroneity illustrated by above examples may imply that the intensification of the southwest monsoon occurred progressively from the monsoon source in the Southern Indian Ocean first to North Africa, West Asia and Southwestern China, and then finally to the Tibetan Plateau. This could be one explanation for the lagged response of the plateau to the Indian monsoon. Another possible factor may be the high altitude and snow cover of the plateau, which may have delayed the response to climate warming.

The intensification of monsoon in the early Holocene

The Indian monsoon was most enhanced between 9.0 and 6.0 ka as a result of solar radiation variations in the northern hemisphere (Kutzbach and Street-Perrott, 1985; COHMAP members, 1998). Large-scale lake expansion occurred then on the Tibetan Plateau (Wang and Wang, 1992). Similarly, deposits in the Arabian Sea show that the most intense period was 8.85 to 7.85 ka (Sirocko et al., 1993). Inconsistently, the glacial lake on Yuju Peak became shallow under a dry climate during this otherwise wet period. This may have resulted from a "sensible heat driven air pump" (SHAP), a feature of the Tibetan Plateau. SHAP pumps moisture to the inner plateau from marginal areas. Therefore, precipitation is reduced on the Diancang Massif and other mountains in the southeast part of the plateau (Wu, 2004).

A new ice age in the middle Holocene

Indications of a cold, arid environment from 6.0 to 5.3 ka on the Diancang Massif are consistent with the record in lacustrine deposits of Heqing Basin, which is north of the Diancang Massif (Jiang et al., 1998). Such a noteworthy event can also be found in neighboring regions around the plateau, such as in the Hongyuan peat bog in the eastern part of the Plateau (Hong et al., 2003), in the middle of the Kunlun mountains (Huang et al., 1996), in the Minqin Basin northeast of the Plateau (Chen et al., 2001), in the Qilian mountains on the northeastern margin of the plateau (Wu et al., 2000), and in Zoige Basin on the eastern margin of the Plateau (Liu et al., 1995). As a cold source in Middle Asia, the Tibetan Plateau is sensitive to any reduction in isolation. Phadtare, (2000) integrated considerable evidence, including glacial advances and changes in lake and sea levels, and suggested a weakened southwest monsoon on the Plateau and neighboring regions around this period. Lake records in the African and other Indian monsoon domains (DeMenocal et al., 2000b; Gasse, 2000; Enzel et al., 1999) suggest that monsoon precipitation decreased abruptly between 6 and 5 ka. With glacier advances in other regions in the northern hemisphere, this period is considered to be a new ice age during which the Siberian High is strengthened and shifted southwards (Denton, 1973).

In contrast to other regions, the Diancang Massif was wetter after ~5.3 ka. One factor related to this difference is a trough in the

https://doi.org/10.1016/j.yqres.2009.11.004 Published online by Cambridge University Press

southward-shifted westerlies during ice ages. This trough passes over the Bay of Bengal and brings moisture from the bay to the southeastern part of the Plateau. The glaciers on Diancang might benefit from increased precipitation in the spring and autumn during such a cold period.

The arid stage in the late Holocene

As a resulting of the orbitally-induced lowering of summer insolation and the southward shift of the ITCZ, a broad decline in Asian monsoon intensity through the latter part of the Holocene correlates well with other northern low-latitude records (Wang et al., 2005). This period of weakened monsoon is dated to 4.5 to 5 ka by Morrill et al. (2003). However, it seems that across the Plateau this weakening starts a little later than in most of the other regions. The record of reddened sediment from Qinghai Lake documents a dry period starting about 4.2 ka (Ji et al., 2005). Evidence in the Tibetan Plateau indicates that levels in most lakes fall 20–40 m abruptly between 4.0 and 3.0 ka (Fang, 1991; Zhang et al., 1998). This late drying phase is also shown by deposits in other lakes, such as Silling Co (after 4.2 ka, Gu et al., 1993), Bangong Co (3.9–3.2 ka, Gasse et al., 1991) and Qaidam basin (4.0~3.0 ka, Zhang et al., 1998).

As the mechanism for this weakening of the monsoon is still not clear (Morril et al., 2003), further discussion of the delay on the Tibetan Plateau is unwarranted and more correlations and numerical simulations are needed. However, one possible reason for aridity in the southeastern Tibetan Plateau could be the strengthening and westward stretching of the Subtropical High in the West Pacific Ocean, which impedes the flow of the Indian Monsoon to the southeast of the Hengduan Mountains, resulting in a shortage of moisture transport to the Plateau. Related evidence is the recorded high lake levels at 3.0 ka in the middle and lower reaches of the Yangtze River (Wang and Wang, 1992). This was caused by the Subtropical High stagnating around 20–25°N latitude, leading to greatly increased rainfall in northern areas (Yang and Sun, 2003; Wei et al., 2004).

Conclusions

The land–sea correlation of Indian monsoon variability and its regional features on the southeastern margin of the Tibetan Plateau after the last glacial period is proposed in this study. Based on the lacustrine deposits, glacial stillstands, and records of human activities, six climate stages can be identified during the Holocene on the Diancang Massif. Stage I, from 11.5 to 9.0 ka, represents the onset of the Holocene and is characterized by warm, wet conditions; from 9.5 to 6.0 ka, the climate turned drier; a cold period followed from 6.0 to 5.3 ka and was succeeded by a temperate, wet period from 5.3 to 4.0 ka; a dry climate returns from 4.0 to 0.73 ka, at which time a warm, wet stage started. This study suggests that the response of the regions around Tibetan Plateau to the Indian monsoon is later than in regions closer to the Indian Ocean. The climate on the Diancang Massif becomes exceptionally dry as the Indian monsoon intensifies during the early Holocene. Another difference on the Diancang Massif is a temperate, wet period from 5.3 to 4.0 ka, which is attributed to a trough in the southward-shifted westerlies. This trough brought considerable moisture from the Bay of Bengal.

Acknowledgments

This research is funded by the National Natural Science Foundation China (Grant No. 40701017 and No. 40801006) and CAS KZCX2-YW-104. The authors express their most sincere appreciation to the Construction Bureau of Dali State, Yunnan Province. We would like to extend their special thanks to Dr. Roger Hooke for suggestions and language corrections. The authors are thankful to two reviewers for their critical remarks.

References

Bookhagen, B., Fleitmann, D., Nishiizumi, K., Strecker, M.R., Thiede, R.C., 2006. Holocene monsoonal dynamics and fluvial terrace formation in the northwest Himalaya, India. Geology 34 (7), 601–604.
Chen, Q., Zhao, W., 1997. Aerial images observation of glacial landforms at Diancang Mt., Dali, Yunnan. Yunnan Geographic Environment Research 9 (2), 66–73 (in Chinese with English Abstract).
Chen, F., Zhu, Y., Li, J., Shi, Q., Jin, L., 2001. Abrupt Holocene changes of the Asian monsoon at millennial-and centennial-scales: evidence from lake sediment document in Minqin Basin, NW China. Chinese Science Bulletin 46 (23), 1942–1947.
Chen, J., Wan, G., David, D., Zhang, F., Huang, R., 2004. Environmental records of lacustrine sediments in different time scales: sediment grain size as an example. Science in China (Series D) 47 (10), 954–960.
COHMAP members, 1998. Climate changes of the last 18ka: observations and model simulations. Science 241, 1043–1052.
Credner, W., 1932. Observation on Geology and Morphology of Yunnan. Geology Survey of Kwangtung and Kwangshi. Special Publications, p. 51.
DeMenocal, P., Ortiz, J., Guilderso, T, 2000a. Coherent High- and Low-Latitude Climate Variability During the Holocene Warm Period. Science 288, 2198–2202.
DeMenocal, P., Ortiz, J., Guilderso, T, 2000b. Abrupt onset and termination of the African Humid Period: rapid climate responses to gradual insolation forcing. Quaternary Science Review 19, 347–361.
Denton, G.A., 1973. Holocene climatic variations: their pattern and possible cause. Quaternary Research 3, 155–205.
Duan, C., 1995. The climate of Cangshan. In: Duan, C. (Ed.), Scientific investigation of the plant on cangshan mountain. Science and Technology Press, Kunming, Yunnan, pp. 14–38 (in Chinese).
Dykoski, C.A., Edwards, R.L., Cheng, H., Yuan, D., Cai, Y., Zhang, M., Lin, Y., Qing, J., An, Z., Revenaugh, J., 2005. A high-resolution, absolute-dated Holocene and deglacial Asian monsoon record from Dongge Cave, China. Earth and Planetary Science Letters 233, 71–86.
Enzel, Y., Ely, L.L., Mishra, S., Ramesh, R., Amit, R., Lazar, B., Rajaguru, S.N., Baker, V.R., Sandler, A., 1999. High-resolution Holocene environmental changes in the Thar Desert, Northwestern India. Science 284 (5411), 125–128.
Fang, J.Q., 1991. Lake evolution during the past 30,000 years in China, and its implications for environmental change. Quaternary Research 36, 37–60.
Gasse, F., 2000. Hydrological changes in the African tropics since the Last Glacial Maximum. Quaternary Science Reviews 19, 189–211.
Gasse, F., Arnold, M., Fonts, J.C., Fort, M., Gilbert, E., Huc, A., Li, B., Li, Y., Liu, Q., Méliéres, F., Van, C.E., Wang, F., Zhang, Q., 1991. A 13,000-year climate record from western Tibet. Nature 353, 742–745.
Gu, Z., Liu, J., Yuan, B., An, K., 1993. The changes in monsoon influence in the Qinghai-Tibetan Plateau during the past 12000 years—geochemical evidence from Silling Co sediments. Chinese Science Bulletin 38, 61–64.
Herzschuh, U., 2006. Palaeo-moisture evolution in monsoonal Central Asia during the last 50,000 years. Quaternary Science Reviews 25, 163–178.
Hong, Y.T., Hong, B., Lin, Q.H., 2003. Correlation between Indian Ocean summer monsoon and North Atlantic climate during the Holocene. Earth and Planetary Science Letters 211, 371–380.
Huang, C.X., Van, C.E., Li, S.K., 1996. Holocene environmental changes of western and northern Qinghai-Xizang Plateau based on pollen analysis. Acta Micropalaeontologica Sinica 13 (4), 423–432 (in Chinese, with English abstract).
IB-CAS (Institute of Botany, Chinese Academy of Sciences), 1976. Spore Pteridophytorum Sinicorum. Science Publication, Beijing, p. 451.
IBSCIB-CAS (Institute of Botany and South China Institute of Botany, Chinese Academy of Sciences), 1982. Angiosperm Pollen Flora Of Tropical and Subtropical China. Science Press, Beijing, p. 453.
Jiang, X.Z., Wang, S.M., Yang, X.D., 1998. Paleoclimatic and environmental changes over the last 30,000 years in Heqing basin, Yunnan province. Journal of Lake Sciences 10 (2), 10–16 (in Chinese, with English abstract).
Ji, J., Shen, J., Balsam, W., Chen, J., Liu, L., Liu, X., 2005. Asian monsoon oscillations in the northeastern Qinghai–Tibet Plateau since the late glacial as interpreted from visible reflectance of Qinghai Lake sediments. Earth and Planetary Science Letters 233, 61–70.
Kutzbach, J.E., Street-Perrott, F.A., 1985. Milankovitch forcing of fluctuations in the level of tropical lakes from 18 to 0 kyr BP. Nature 317, 130–134.
Leuschner, D.C., Sirocko, F., 2003. Orbital insolation forcing of the Indian Monsoon—a motor for global climate changes? Palaeogeography, Palaeoclimatology, Palaeoecology 197, 83–95.
Liu, G.X., Shen, Y.P., Wang, S.M., 1995. The vegetation and climate of Holocene Megathermal in Zoige, Northwestern Sichuan, China. Journal of Glaciology and Geocryology 17 (3), 247–249 (in Chinese, with English abstract).
Liu, K., Guo, Z., Lu, X., 2000. Improvements of PKUAMS for precision 14C analysis of the project of Xia-Shang-Zhou chronology. Nuclear Instruments and Methods in Physics Research-B 172, 70–74.
Luo, J.Y., Chen, Z.D., 1998. Paleo-environmental records from the elemental distribution in the sediments of great ghost lake in Taiwan, China. Journal of Lake Sciences. 10 (3) 13-18 (in Chinese, with English abstract).
Moore, P.D., Webb, J.A., Collison, M.E., 1991. Pollen Analysis, 2nd ed. Blackwell Science, Oxford.
Moore, P.D., Webb, J.A., Collinson, M.E., 1999. Pollen analysis. Black- 1319 well, Oxford.
Morrill, C., Overpeck, J.T., Cole, J.E., 2003. A synthesis of abrupt changes in the Asian summer monsoon since the last deglaciation. The Holocene 13 (4), 465–476.
Phadtare, N.R., 2000. Sharp decrease in summer monsoon strength 4000–3500 cal yr B.P. in the Central Higher Himalaya of India based on pollen evidence from Alpine Peat. Quaternary Research 53, 122–129.

https://doi.org/10.1016/j.yqres.2009.11.004 Published online by Cambridge University Press

Shen, J., Yang, L., Yang, X., 2005a. Lake sediment records on climate change and human activities since the Holocene in Erhai catchment, Yunnan Province, China. Science in China, Ser. D 48 (3), 353363.
Shen, J., Liu, X.Q., Matsumoto, R., Wang, S., Yang, X., 2005b. A high-resolution climatic change since the Late Glacial Age inferred from multi-proxy of sediments in Qinghai Lake. Science in China, Ser. D. 48 (6), 742–751.
Sirocko, F., Sernthein, M., Erlenkeuser, H., Lange, H., Arnold, M., Duplessy, J.C., 1993. Century-scale events in monsoonal climate over the past 24,000 years. Nature 364, 322–324.
Tan, H.B., Yu, S.S., 1999. Present distribution and future development of elemental geochemistry in the study of lake sediments' evolution. Journal of Salt Lake Research 7 (3), 59–65 (in Chinese, with English abstract).
Thompson, L.G., Thompson, E.M., Davis, M.E., Mashiotta, T.A., Henderson, K.A., Lin, P.N., Yao, T., 2006. Ice core evidence for asynchronous glaciation on the Tibetan Plateau. Quaternary International. 154-155, 3–10.
Wang, F.X., Chen, N.F., Zhang, Y.L., Yang, H.Q., 1995. Pollen Flora of China. Science Publications, Beijing, p. 461.
Wang, S.M., Wang, F.B., 1992. The liminogic record of Holocene climate fluctuation. In: Shi, Y.F. (Ed.), The climates and environments of Holocene Megathermal in China. China Ocean Press, Beijing, pp. 146–152 (in Chinese, with English abstract).
Wang, Y., Cheng, H., Edwards, R.L., He, Y., Kong, X., An, Z., Wu, J., Kelly, M., Dykoski, C.A., Li, X., 2005. The Holocene Asian Monsoon: links to solar changes and North Atlantic climate. Science 308, 854–858.
Wan, Y., Han, T., Duan, C., Yang, H., 2005. Landform system structures and characteristics of the DiancangMountain Areas in West Yunnan Province. Journal of Glaciology and Geocryology 27 (2), 241248 (in Chinese with English Abstract).
Wei, J., Yang, H., Sun, S.Q., 2004. Relationship between the anomaly longitudinal position of subtropical high in the western Pacific and severe hot weather in north China in summer. Acta Meteorologica Sinica 62 (3), 308–316 (in Chinese, with English abstract).
Writing Group of Yunnan Vegetation, 1987. Vegetation of Yunnan. Science Press, Beijing, p. 843. in Chinese.
Wu, G., 2004. Recent progress in the study of the Qinghai-xizang Plateau. Quaternary Sciences 24 (1), 1–13 (in Chinese, with English abstract).
Wu, G., Pan, B., Guang, Q., Liu, Z., Wang, Y., 2000. Study on Hydro-Thermal Characteristic of Eastern Qilian Mountains in Holocene and Present. Scientia Geographica Sinica 20 (2), 160–165 (in Chinese, with English abstract).
Wu, X., Sun, H., Liu, Y., 2000a. The conformation alternation of mouse hepatic histones after reacting with nicotine *in vitro*. Chinese Science Bulletin 45 (9), 825–829.
Wu, X., Yuan, S., Guo, Z., 2000b. Chronological research of mausoleums of Jin Seigneurs in China by 14C-AMS. Nuclear Instruments and Methods in Physics Research-B 172, 732–735.
Wu, Y., Lücke, A., Jin, Z., Wang, S., Schleser, G.H., Battarbee, R.W., Xia, W., 2006. Holocene climate development on the central Tibetan Plateau: a sedimentary record from Cuoe Lake. Palaeogeography, Palaeoclimatology, Palaeoecology 234, 328–340.
Yang, H., Sun, S.Q., 2003. Study on the characteristics of longitudinal movement of subtropical high in the western Pacific in summer and its influence. Advances in Atmospheric Sciences 20 (6), 921–933 (in Chinese, with English abstract).
Yang, J, Zhang W., Cui, Z., Yi C. & Liu, K, 2006, Late Pleistocene glaciation of the Diancang and Gongwang Mountains, southeast margin of the Tibetan plateau. Quaternary International. 154-155, 52-62.
Yang, J., Cui, Z., Yi, C., Sun, J., Yang, L., 2007. About "Tali Glaciation" on The Diancang Massif. Science in China Series D-Earth Sciences 50 (11), 1685–1692.
Yang, X.D., Shen, J., Jones, R.T., et al., 2005. Pollen evidence of early human activities in Erhai basin, Yunnan Province. Chinese Science Bulletin. 50 (6), 568–576.
Yuan, S., Wu, X., Gao, S., 2000a. The CO2 Preparation System for AMS Dating at PKU. Nuclear Instruments and Methods in Physics Research-B 172, 458–461.
Yuan, S., Wu, X., Gao, S., 2000b. The selection of components of bone for AMS radiocarbon dating. Nuclear Instruments and Methods in Physics Research-B 172, 424–427.
Zhang, Q., Wang, L., Shen, C., Li, B., Shi, Y., 1998. Main characteristics of the environmental changes on the Qinghai-Xizang (Tibetan Plateau). In: Shi, Yafeng, Li, Jijun, Li, Bingyuan (Eds.), Uplift and Environmental Changes of Qinghai-Xizang (Tibetan) Plateau in the late Cenozoic. Guangdong Science and Technology Press, Guangzhou, p. 345.
Zhang, X.L., 1997. The historical changes of the habitation environment in the area of Cangshan Mountains and Erhai Lake. Environmental Research of Yunnan Province 16 (4), 3–8 (in Chinese, with English abstract).
Zhou, J., Wang, S.M., Lv, J., 2003. Climate and environmental changes from the sediment record of Erhai Lake over the past 1000 years. Journal of Lake Sciences 15 (2), 104–111 (in Chinese, with English abstract).